

The Role of the Interface Reactions in the Electroforming of Redox-based Resistive Switching Devices Using KMC Simulations

Elhameh Abbaspour
Institute of Electromagnetic Theory
RWTH Aachen University
Aachen 52056, Germany
Email: ea@ithe.rwth-aachen.de

Stephan Menzel
Peter Grünberg Institut
Forschungszentrum Jülich
52425 Jülich, Germany
Email: st.menzel@fz-juelich.de

Christoph Jungemann
Institute of Electromagnetic Theory
RWTH Aachen University
Aachen 52056, Germany
Email: cj@ithe.rwth-aachen.de

Abstract—In this paper we apply a physical model based on kinetic Monte Carlo (KMC) simulations to investigate the electroforming process of ReRAMs. In this model the electric current through the oxide is assisted by oxygen vacancies which are generated at the anode-oxide interface and introduced into the oxide. The major driving forces that control these processes are the electric field, temperature and temperature gradient. Transient simulation on short timescales was done to obtain the forming time as a function of the voltage pulse amplitude.

I. INTRODUCTION

Redox-based resistive switching RAM (ReRAM) is currently under consideration as a competitive candidate for future nonvolatile memory application due to its high scalability potential and compatibility with CMOS technology [1]. The switching between high and low resistance states for ReRAMs has been reported to be based on the formation and rupture of conducting filaments (CF) which may consist of oxygen vacancies ($V_{\bar{o}}$) [2], [3]. Typically an initial one-time electroforming process regarded as a soft dielectric breakdown, is required to generate these metal-rich CFs inside the oxide [1]. Despite the major progress in understanding the forming process, several aspects have still to be fully understood [4], [5]. The role of the metal-electrode interface in CF formation [6], [7] is one of these aspects, which is crucial for device operation and reliability.

In this study we developed a KMC model in order to investigate the key aspects of the electroforming process, specifically the electrode dependent CF formation in HfO_2 -based ReRAM. Most of the former KMC models for the electroforming/switching in HfO_x ReRAM are bulk models and interface reactions are neglected. All of them assume that Frenkel defect pairs consisting of oxygen interstitials and oxygen vacancies can be generated within the bulk film [5], [8]–[10]. However, it has been shown that these pairs of defects are energetically unfavorable and not stable [11]–[13]. Here, we present a model where the oxygen vacancies can only be introduced into the system by oxygen exchange at the boundary. With this model similar forming characteristics are observed as with the previous models [8], [10]. Transient simulations are also performed in this

work to study the forming kinetics in HfO_2 -based cells at the forming timescale. In particular, we characterize the forming time as a function of the voltage pulse amplitude.

In Sec. II, the details of the KMC model for simulation of the electroforming process are described. The KMC simulation results are presented and discussed in Sec. III followed by the conclusion.

II. DESCRIPTION OF FORMING MODEL

During the electroforming process a CF connecting one electrode to the other is created. This process is assisted by generation of new $V_{\bar{o}}$ at the anodic interface and migration of them through the oxide. $V_{\bar{o}}$ s play the role of traps where electrons can jump through them and control the leakage current through the oxide. A trap assisted tunneling (TAT) current solver has been developed in this work to calculate the electronic current through HfO_2 , which includes both potential and temperature dependencies of the cell current. Our model considers electron dynamics as following

- electron hop from an electrode into $V_{\bar{o}}$;
- electron hop from $V_{\bar{o}}$ to an electrode;
- electron hop between two $V_{\bar{o}}$.

Direct tunneling is used for hopping between electrodes and traps where the tunneling probabilities are given by the Wentzel–Kramers–Brillouin (WKB) approximation. The electron TAT current flowing through the oxide is defined as the electron flux through one of the electrodes,

$$I_{TAT} = e \sum_{n=1}^N [p_n H_{na} - (1 - p_n) H_{an}] \quad (1)$$

where e is the electron charge, N the total number of traps, p_n the occupational probability of trap n and H_{na} and H_{an} are the rates of an electron hop from trap n to the anode and vice versa calculated by considering a direct tunneling process. In order to calculate the occupational probabilities of the traps, the current continuity equation for the quasi-steady state is solved,

$$(1 - p_n) \sum_{m=1, m \neq n}^N p_m h_{mn} - p_n \sum_{m=1, m \neq n}^N (1 - p_m) h_{nm} \quad (2)$$

$$+(H_{cn} + H_{an})(1 - p_n) - (H_{nc} + H_{na})p_n = 0.$$

with h_{nm} being the hopping rate of electrons from trap n to m in the Miller-Abrahams form.

Fig. 1 shows the simulation flow of the forming process in a two dimensional system with a random initial distribution of V_{δ} along grain boundaries (GB). GBs have been found to be weak links where the oxygen vacancies tend to accumulate around them [8]. The simulation stops when a predefined current compliance is reached. At each loop Poisson and current continuity equations are solved self consistently. Based on electrical current information from the TAT solver the corresponding power dissipation map is obtained which is used to calculate the local temperature by solving the heat flow equation. The derived local potential and temperature are used to calculate the involved transition rates

$$G_i = \nu_0 \exp\left(-\frac{E_G - F_{ext}}{k_B T}\right) \quad (3)$$

$$D_{i,j} = \nu_0 \exp\left(-\frac{E_D - \alpha q(V_i - V_j - V_{self,i}) - k_B a \nabla T}{k_B T}\right). \quad (4)$$

Here, G_i is the new V_{δ} generation rate at point i that belongs to the anodic interface and $D_{i,j}$ is the vacancy hopping rate from site i to site j . ν_0 is the characteristic vibration frequency, k_B is the Boltzmann constant and T is the local temperature. E_G and E_D are the activation energies of generation and hopping. α is the symmetry factor, a is the lattice constant and q is the charge state of the vacancies. The values of the main parameters that we used in the simulation are provided in Table I. F_{ext} is the locally induced electric field by the applied voltage bias. V_i is the solution of the Poisson equation at site i and $V_{self,i}$ is the self potential at this site that should be excluded from V_i . The external applied electric field, electrical potential and temperature gradient are factors that modulate the activation energies. $E_G - F_{ext}$ and $E_D - \alpha q(V_i - V_j - V_{self,i}) - k_B a \nabla T$ represent the effective V_{δ} generation and diffusion activation energies, respectively.

TABLE I. VALUES OF THE MAIN PHYSICAL PARAMETERS USED IN THE ELECTROFORMING SIMULATIONS

ν_0	E_G	E_D	α	k_{th}	ϵ_r
10^{13} Hz	3.0eV	0.7eV	0.5	0.5(W/Km)	25

III. RESULTS AND DISCUSSION

Fig. 2 shows the simulated distribution of newly generated V_{δ} and temperature along the GB during the forming process at different stages of applied ramp voltage to the active electrode with a rate of 1 V/s in a dc sweep. At the final stage (D) a percolation path is created along the GB and the formation process is completed. Fig. 3(a) shows the simulation results of the electron occupation probabilities during forming. The calculated data is used by the TAT solver to obtain the current through CF. The current-voltage traces are demonstrated in Fig. 3(b) and the inset shows the derived current density obtained from these traces. Fig. 4(a) and 4(b) provide the simulation results of V_{δ} density and power dissipation during the

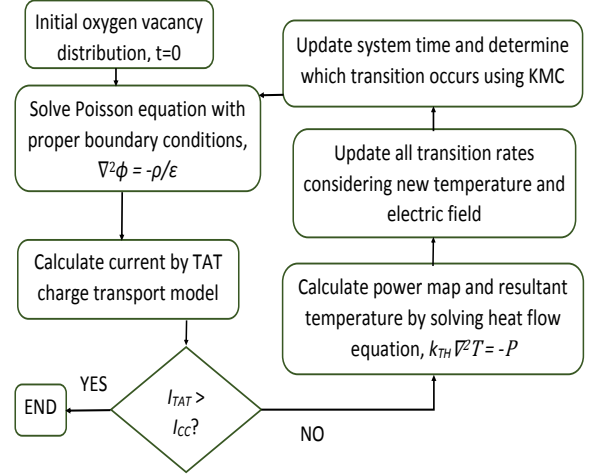


Fig. 1. Flowchart of the KMC simulator developed in this work to study forming process, where I_{cc} is the predefined compliance current.

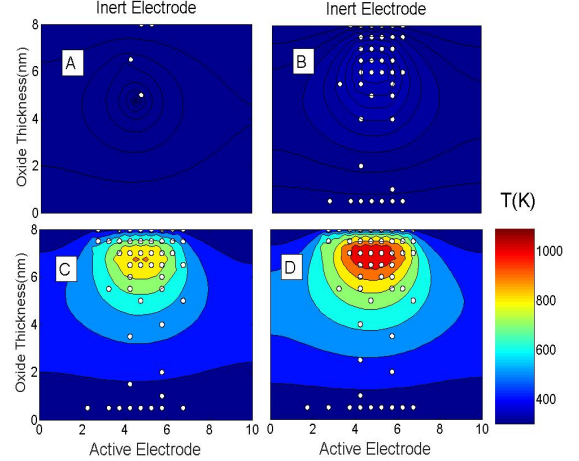


Fig. 2. The evolution of V_{δ} distribution and temperature along CF during the forming process in a TiN/HfO₂(8 nm)/Pt cell at different stages A($V = 0.5$ V), B($V = 3.0$ V), C($V = 4.1$ V), D($V = V_f = 4.3$ V)

forming process inside the percolation path at ambient temperature. The results show the non uniform distribution of V_{δ} inside CF with maximum density close to the inert electrode. The power dissipation is larger close to the inert electrode which results in a higher temperature in this region that can be seen from Fig. 2.

The characteristics of the forming voltage and forming time i.e., the so called “Voltage–time dilemma” is a particular issue in resistive switching devices [14]. The time scale of the electroforming process can be significantly different depending on the voltage sweep rate. The dependency of the forming time and voltage on the voltage sweep rate was investigated as shown in Fig. 5. The results show a significant dependence of the forming time on the voltage sweep rates, and for a change in the sweep rate

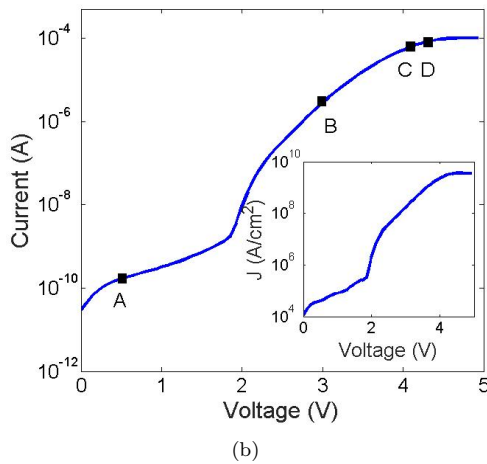
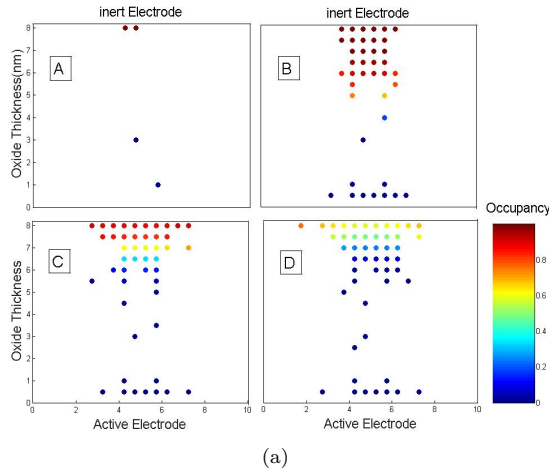


Fig. 3. (a) Calculated distribution of the electron occupation probabilities during the forming process when a ramp up voltage is applied (b) The $I - V$ characteristics from the forming operation calculated by the TAT solver. The inset shows the forming current density inside the cell

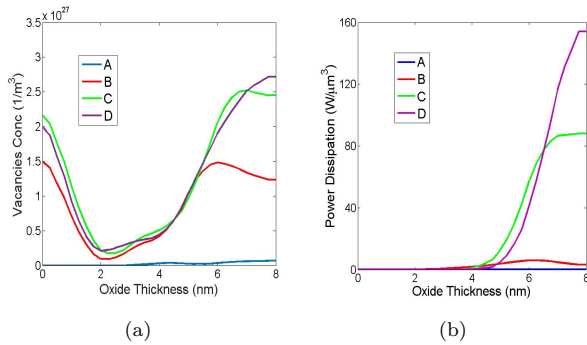


Fig. 4. (a) Simulation results of the calculated V_{δ} density profile inside CF during forming at different stages (A-D). Oxide thicknesses, $x = 0$ and $x = 8 \text{ nm}$ correspond to active and inert electrodes respectively (b) power dissipation as derived from the simulation of the leakage current through CF

from 0.01 to 0.1 V/s the forming time changes by two orders of magnitude. In contrast to the forming time the

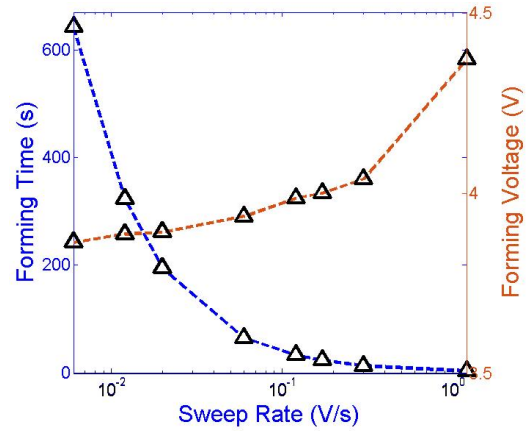


Fig. 5. Dependency of forming time and voltage on the voltage sweep rate

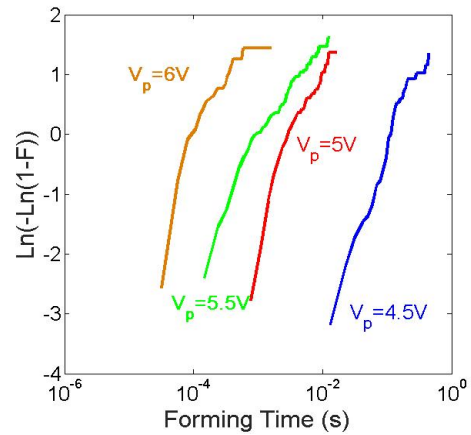


Fig. 6. Weibull plot of the forming time for different applied pulse amplitudes

forming voltage does not significantly change with the sweep rate. This might be due to the high activation energy for V_{δ} generation, which leads to a low probability for V_{δ} generation unless its threshold voltage is exceeded.

We also performed transient simulations for extremely short durations of the voltage pulse to investigate the influence of the applied voltage pulse amplitude on the forming time. The amplitudes of the applied voltage pulses are all greater than the average value of the forming voltage of the sweep simulations which is 4.3 V. The results in Fig. 6 show a trade-off between voltage down scaling and fast programming due to a significant increase of the forming time when the voltage amplitude is reduced. For example, for a voltage decrease of 25% the forming time increases by about two orders of magnitude.

In order to understand the effect of the interface reactions on the switching characteristics we simulated the forming process for different V_{δ} formation energies (E_G) at the anodic interface. Fig. 7(a) and 7(b) demonstrate the simulation results of the $I - V$ characteristics and the

ACKNOWLEDGMENT

This work was supported by the Deutsche Forschungsgemeinschaft under Grant SFB 917.

REFERENCES

- [1] R. Waser, R. Dittmann, G. Staikov, and K. Szot, "Redox-Based Resistive Switching Memories – Nanoionic Mechanisms, Prospects, and Challenges," *Advanced Materials*, vol. 21, no. 25-26, pp. 2632–2663, 2009.
- [2] K. M. Kim, B. J. Choi, Y. C. Shin, S. Choi, and C. S. Hwang, "Anode-interface localized filamentary mechanism in resistive switching of TiO₂ thin films," *Applied Physics Letters*, vol. 91, no. 1, 2007.
- [3] E. Miranda, C. Walczyk, C. Wenger, and T. Schroeder, "Model for the Resistive Switching Effect in HfO₂ MIM Structures Based on the Transmission Properties of Narrow Constrictions," *Electron Device Letters, IEEE*, vol. 31, no. 6, pp. 609–611, 2010.
- [4] P. Gonon, M. Mougnot, C. Vallée, C. Jorel, V. Jousseau, H. Grampeix, and F. El Kamel, "Resistance switching in HfO₂ metal-insulator-metal devices," *Journal of Applied Physics*, vol. 107, no. 7, 2010.
- [5] B. Butcher, G. Bersuker, D. Gilmer, L. Larcher, A. Padovani, L. Vandelli, R. Geer, and P. Kirsch, "Connecting the physical and electrical properties of Hafnia-based RRAM," *Electron Devices Meeting (IEDM), 2013 IEEE International*, pp. 22.2.1–22.2.4, 2013.
- [6] L. Zhang, R. Huang, M. Zhu, S. Qin, Y. Kuang, D. Gao, C. Shi, and Y. Wang, "Unipolar TaOx-Based Resistive Change Memory Realized With Electrode Engineering," *Electron Device Letters, IEEE*, vol. 31, no. 9, pp. 966–968, 2010.
- [7] A. Padovani, L. Larcher, P. Padovani, C. Cagli, and B. De Salvo, "Understanding the Role of the Ti Metal Electrode on the Forming of HfO₂-Based RRAMs," *Memory Workshop (IMW), 2012 4th IEEE International*, pp. 1–4, 2012.
- [8] G. Bersuker, D. C. Gilmer, D. Veksler, P. Kirsch, L. Vandelli, A. Padovani, L. Larcher, K. McKenna, A. Shluger, V. Iglesias, M. Porti, and M. Nafria, "Metal oxide resistive memory switching mechanism based on conductive filament properties," *Journal of Applied Physics*, vol. 110, no. 12, 2011.
- [9] L. Vandelli, A. Padovani, L. Larcher, G. Broglia, G. Ori, M. Montorsi, G. Bersuker, and P. Pavan, "Comprehensive physical modeling of forming and switching operations in HfO₂ RRAM devices," *Electron Devices Meeting (IEDM), 2011 IEEE International*, pp. 17.5.1–17.5.4, 2011.
- [10] X. Guan, S. Yu, and H.-S. Wong, "On the Switching Parameter Variation of Metal-Oxide RRAM; Part I: Physical Modeling and Simulation Methodology," *Electron Devices, IEEE Transactions on*, vol. 59, no. 4, pp. 1172–1182, 2012.
- [11] A. O'Hara, G. Bersuker, and A. A. Demkov, "Assessing hafnium on hafnia as an oxygen getter," *Journal of Applied Physics*, vol. 115, no. 18, 2014.
- [12] S. Clima, B. Govoreanu, M. Jurczak, and G. Pourtois, "HfOx as RRAM material – First principles insights on the working principles," *Microelectronic Engineering*, vol. 120, pp. 13 – 18, 2014.
- [13] Y. Guo and J. Robertson, "Materials selection for oxide-based resistive random access memories," *Applied Physics Letters*, vol. 105, no. 22, 2014.
- [14] S. Menzel, U. Böttger, M. Wimmer, and M. Salinga, "Physics of the Switching Kinetics in Resistive Memories," *Advanced Functional Materials*, 2015.

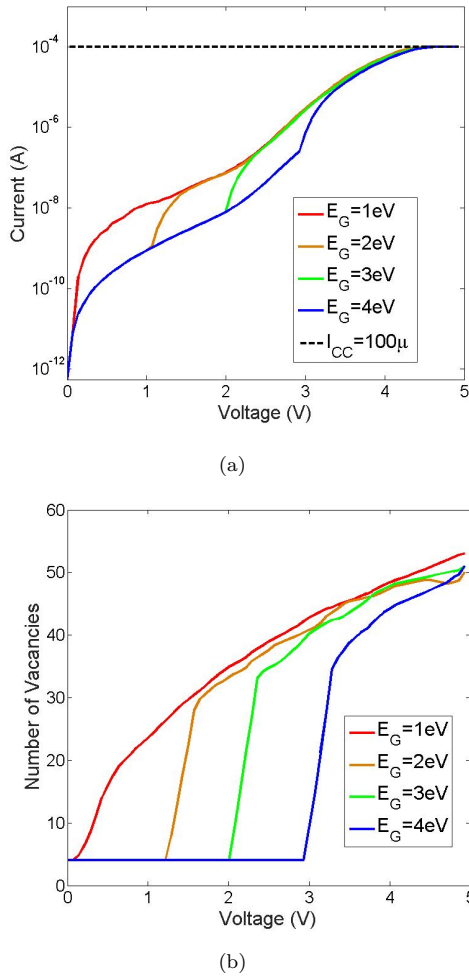


Fig. 7. (a) Simulation results of $I - V$ curves and (b) number of V_{δ} during forming process for different V_{δ} formation energy

evolution of the number of V_{δ} during the voltage ramp with a sweep rate of 1 V/s. Our results show the increase of current and number of V_{δ} by decreasing the V_{δ} formation energy in the pre-forming state. After a specific increase of voltage all curves follow the same trace because of the similar vacancy distribution profile along CF.

IV. CONCLUSION

A KMC approach has been presented to investigate the CF formation in a HfO₂-based ReRAM, in which oxygen vacancies can only be introduced at the anodic interface and not within the bulk. Our model produced similar forming characteristics as previous models. Studying the forming kinetics elucidated the influence of voltage pulse amplitude and voltage sweep rate on the forming time and voltage. Forming time and voltage change significantly with voltage sweep rate. The forming time increases with increasing the voltage pulse amplitude.